

Article

Effect of Bias Voltage on Microstructure and Properties of Tantalum Nitride Coatings Deposited by RF Magnetron Sputtering

Wei Dai * and Yunzhan Shi

School of Electromechanical Engineering, Guangdong University of Technology, Guangzhou 510006, China; 2112001057@mail2.gdut.edu.cn

* Correspondence: weidai@gdut.edu.cn; Tel.: +86-20-39322212

Abstract: TaN_x coatings were deposited by RF magnetron sputtering with different bias voltages. The growth morphology, crystalline structure, chemical bond structure, hardness and elastic modulus, adhesion strength and tribological performance of the coatings were studied as a function of the bias voltage. The results showed that an increasing bias voltage refines the coating grains and facilitates structure densification. Simultaneously, the structure of the TaN_x coatings transfers from a composite structure consisting of TaN and Ta₂N crystals, through a single composite mainly composed of the Ta₂N crystal, to an amorphous structure as the bias voltage increases from low to high, indicating that the phase composition of the TaN_x coatings can be varied by the bias voltage. The coating composed of Ta₂N crystal showed a good overall performance including enhanced hardness, enhanced adhesive strength, and good tribological performance with enhanced wear resistance and a low friction coefficient of 0.18.



Citation: Dai, W.; Shi, Y. Effect of Bias Voltage on Microstructure and Properties of Tantalum Nitride Coatings Deposited by RF Magnetron Sputtering. *Coatings* **2021**, *11*, 911. <https://doi.org/10.3390/coatings11080911>

Academic Editor: Diego Martinez-Martinez

Received: 25 June 2021
Accepted: 27 July 2021
Published: 29 July 2021

Publisher's Note: MDPI stays neutral with regard to jurisdictional claims in published maps and institutional affiliations.



Copyright: © 2021 by the authors. Licensee MDPI, Basel, Switzerland. This article is an open access article distributed under the terms and conditions of the Creative Commons Attribution (CC BY) license (<https://creativecommons.org/licenses/by/4.0/>).

Keywords: tantalum nitride; RF sputtering; structure; hardness; tribology

1. Introduction

Tantalum nitride (TaN_x) coating is attracting increasing attention due to its high hardness, high corrosion resistance, good tribological properties and chemical inertness; and thus, TaN_x coating has been extensively used in the microelectronic industry as diffusion barriers and thin coating resistors [1–3]. Usually, TaN_x coatings are deposited by the physical vapor deposition (PVD) (e.g., reactive magnetron sputtering using a Ta target in a N₂/Ar gas mixture [4]). However, TaN_x coating synthesized by reactive magnetron sputtering shows a variety of the stoichiometry, such as Ta₂N, TaN, Ta₄N₅, and Ta₅N₆, due to its defective structure, i.e., high vacancy concentrations of atomic lattice sites can be present during the synthesis of TaN_x thin coatings [5–8]. It is believed that the chemical composition and crystalline structure of the as-deposited TaN_x coatings strongly depend on the deposition technique and the process parameters, such as sputtering power source (e.g., DC [4], RF [9], pulsed power [10]), N₂/Ar ratio [11], bias voltage [12], substrate temperature [13], pressure [14] in the growth chamber, etc.

RF magnetron sputtering is capable of depositing a more uniform and stable coating free of dislocations and crystallographic imperfections compared with other conventional magnetron sputtering (e.g., DC magnetron sputtering). Tan et al. [15] carried out a study to compare the chromium nitride coatings deposited by DC and RF magnetron sputtering, and found that the CrN_x coatings showed optimized microstructure (dense structure) and properties (high hardness) due to the improved plasma density and ion bombardment from the RF condition. In fact, numerous researchers have used RF sputtering to prepare TaN_x coatings and also studied the influences of the process parameters such as N₂ partial pressure [16] and input power [9] on the growth, structure and properties of the coatings. Bias voltage applied on the substrate holder has been considered as an effective approach

to enhance the delivered energy to the growing coatings and the mobility of adatoms and hence promotes densification of structure as well as grain-refining of the coatings [17]. Meymian et al. [18] studied the influence of the bias voltage (0~−250 V) on the Cu₃N films deposited by RF magnetron sputtering and found that the grain sizes decreased and the surface morphology of the films became smoother as the bias voltage increased. It is clear that optimizing the bias voltage is one of the best ways to improve the structure and properties of the coatings. Kuo et al. [12] prepared TaN_x coatings by RF magnetron sputtering with bias voltage ranging from 0 to −200 V and found that the bias voltage has a significant effect on the coating composite (TaN, Ta₂N and β-Ta phases appeared and/or coexisted in the films at specific biases). However, the influences of the bias voltage on the mechanical and tribological properties of the TaN_x coatings were absent.

In this paper, TaN_x coatings were deposited by RF magnetron sputtering with different bias voltages applied on the substrates. The influences of the bias voltage on the structure, hardness and elastic modulus, adhesion strength, tribological performance of the coatings were studied systematically. The relationships between the deposition process, structure and properties were discussed carefully. It is worth noting that, besides N₂ partial pressure, the bias voltage is one of the effective ways to control the phase structure of the TaN_x coatings.

2. Materials and Methods

Series of TaN_x coatings were deposited on the silicon wafers and well-polished stainless steel (SU304) sheets by the RF magnetron sputtering with using Ar/N₂ mixture to sputter Ta target (purity 99.99%, 60 mm in diameter). The substrate is about 10 cm distant from the target. An ultrasonic bath with acetone and ethanol was used to clean the substrates for 10 min. Then the substrates were dried in N₂. The chamber was evacuated to 5×10^{-3} Pa and simultaneously heated up to 300 °C. This temperature was further maintained until the end of the coating process. DC glow discharge with a bias voltage of −700 V was used to etch the substrates for 10 min. Subsequently, in order to improve the adhesion of the TaN_x coatings, 200 nm Ta interlayer was deposited on the substrates by sputtering the Ta target. Before the coating process, pre-sputtering was performed for 5 min to remove any impurities on the target surface. During the coating process, a gas mixture of Ar and N₂ (Ar/N₂ = 30/30 sccm) was introduced into the chamber as the sputtering gas. The deposition pressure was kept around 0.5 Pa. The rotation speed of the substrate holder was set at 1.0 rpm. RF power (RFK30ZC-SW5, Kyosan, Yokohama, Japan) was used for the sputtering process. The RF power was set at approximately 200 W. The bias voltage ranged from 0 V (floating) to −300 V. The deposition duration was 2 h.

Scanning electron microscopy (SEM, Hitachi S-4800, Tokyo, Japan) was used to observe the surface topography and cross-sectional images of the TaN_x coatings. X-ray diffraction (XRD, D8-Discovery Bruker, Karlsruhe, Germany) with 1.54 Å Cu Kα radiation was employed to examine the crystal structure of the TaN_x coatings under an asymmetric model. X-ray photoelectron spectroscopy (XPS, Thermo ESCALAB 250Xi, Waltham, MA, USA) with Al (mono) Kα (hν = 1486.6 eV) was applied to characterize the coating chemical composition and chemical bonds with a step size of 1 eV. The high-resolution XPS spectra with a step size of 0.05 eV were also taken for the coatings. Before the XPS measurement, the sample surface was etched by an Ar⁺ ion beam with an energy of 2 kV for 300 s (the etch depth was about 10 nm) to remove contaminants and oxide on the coating surface. The contents of the coating elements were calculated from the relative area ratios of the peaks in the XPS spectra divided by the corresponding atomic sensitivity factors.

Nano-indentation (CSM, NHT², Anton Paar, Graz, Austrian) with the Berkovich diamond indenter was used to measure the hardness and elastic modulus of the TaN_x coatings using a constant load of 5 mN. In order to eliminate the effect of the soft substrate, the maximum indentation depths were chosen around 1/10th of the coating thicknesses. Each sample was tested 15 times to reduce errors. The coating adhesion strength was tested by a Nano Scratch Tester (CSM, Revetest scratch tester, Anton Paar, Graz, Austrian) using Rockwell C diamond styli with radius 200 μm with a normal load ranging from 1 to

100 N. The scratch length and scratch speed were 3 mm and 6 mm/min, respectively. An optical microscope (Leica DM2500 M, Wetzlar, German) was used to observe the scratch after the scratch test. A ball-on-plate tribometer (CSM, THT, Anton Paar) was employed to measure the tribological performances of the TaN_x coatings with a rotational speed of 200 r/min under a load of 1 N (the initial Hertzian contact pressure was about 0.2 GPa) at room temperature and relative humidity of $50\% \pm 5\%$ conditions. SU304 balls (6 mm in diameter) were used as the counterpart material. The total wear durations were 60 cycles and 300 cycles for one sample. After the tests, the wear tracks were measured by using a laser scanning confocal microscope (OLS4100, Olympus, Tokyo, Japan). In addition, energy dispersive X-ray spectroscopy (EDX) mapping was also carried out on the wear track to detect the composition of the tribological layer.

3. Results and Discussion

Figure 1 shows the surface topographies and cross-sectional morphologies of the TaN_x coatings deposited with different bias voltages. The TaN_x coating deposited at 0 V (Figure 1a,e) shows a coarse columnar structure and granular surface. It can be seen that there are numerous crevices between the columnar and granular structures. As the bias voltage increases, it should be noted that the columnar and granular size show a remarkable decrease, implying that the size of the columnar crystal decreases. Additionally, the crevices are degenerating and the coating structure is getting compact with increasing bias voltage. These results are consistent with the results reported in the literature [19]. An increasing bias voltage would improve the mobility of adatoms and refine the columnar grains. Simultaneously, the increase of the bias voltage would enhance the bombardment effect which contributes to remove defects and facilitates structure densification. However, the increase of the bias voltage also would increase the so-called “self-sputtering” effect that causes the etching of the coating surface [12]. As a result, the thickness of the coatings was decreasing with increasing bias voltage, as shown in the cross-sectional images of Figure 1e–g.

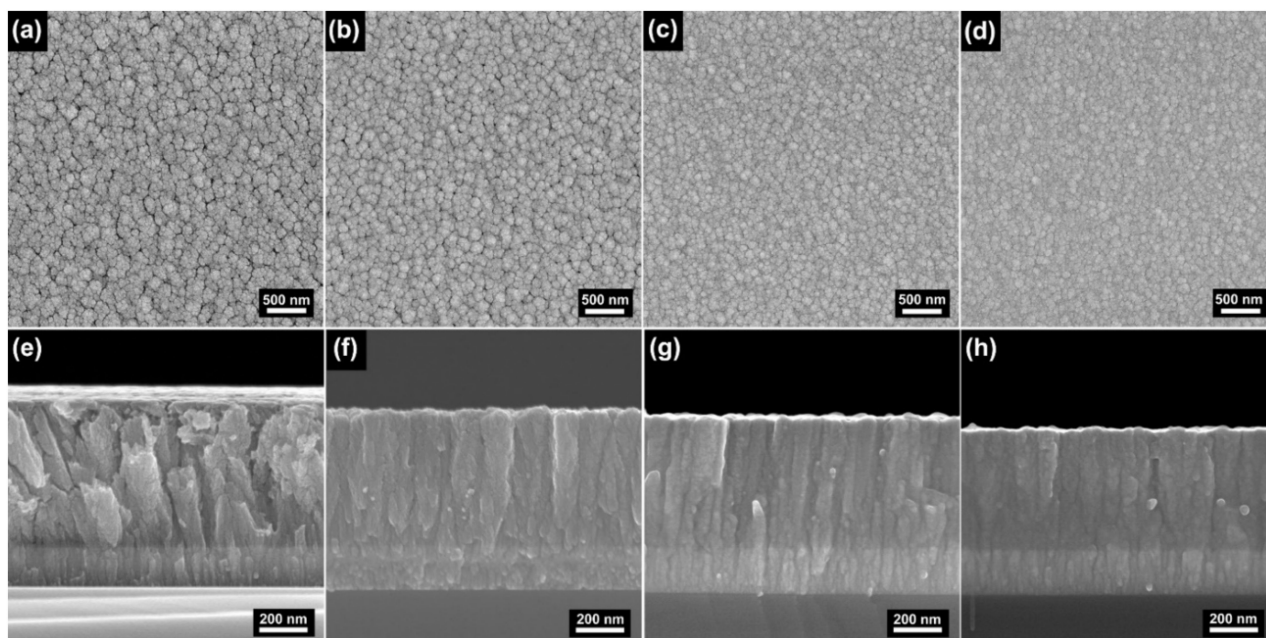


Figure 1. (a–d) Typical surface morphologies of the TaN_x coatings deposited with different bias voltages: (a–d) are 0 V, –100 V, –200 V and –300 V, respectively. (e–h) The corresponding cross section morphologies of (a–d).

The evolution of the Ta, N and O contents and the N/Ta ratio in the TaN_x coatings are presented in Figure 2 as a function of the bias voltage. It can be seen that the Ta and N contents show a slow growth as the bias voltage increases. The N/Ta ratio also increases slowly with the bias voltage. It is supposed that an increasing bias would enhance the

nitrogen doping in the coatings. Oxygen was detected in the coatings and the content decreases with the bias voltage. There are two main reasons for the existence of oxygen in the coatings. Firstly, the residual oxygen in the chamber due to the relatively high base pressure would cause the introduction of oxygen in the coatings. Secondly, the existence of oxygen might be mainly attributed to the exposure of the samples before the XPS test. As shown in the SEM images of Figure 1, the coating deposited at 0 V has a loose and porous structure. The oxygen can be absorbed on these defects. Accordingly, the oxygen content is very high in the XPS test even after etching by Ar^+ beam for 300 s. As the bias voltage increases, the coating structure became compact and dense, reducing the phenomenon of oxygen adsorption.

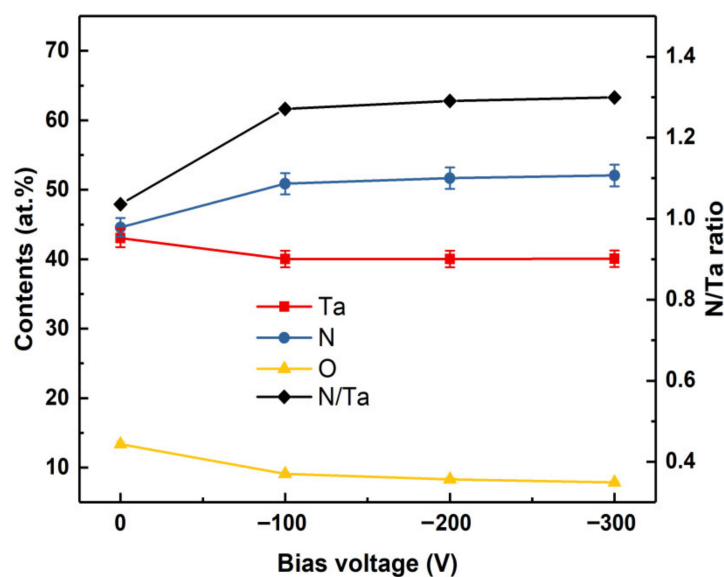


Figure 2. Component contents (by XPS) of the TaN_x coatings as a function of the bias voltages.

Figure 3 shows the XRD patterns of the TaN_x coatings deposited with different bias voltages. The XRD pattern of the coating deposited at 0 V presents diffraction peaks at 2θ angles of 33.7° , 35.5° , 41.6° , which can be identified as the TaN (110), (111) and (200). It is worth noting that there is a peak around 38.2° , which can be identified as the (002) plane of Ta_2N . This indicates that the coating is mainly consisting of TaN and Ta_2N crystals. As the bias voltage increases to -100 V, the diffraction peaks of the coatings become stronger and shaper, implying that the crystallinity of the coatings is enhanced. It is believed that the bias voltage can enhance the delivered energy to the growing coatings and the mobility of adatoms and hence improves the crystallinity of the coatings. As the bias voltage increases to -200 V, the diffraction peaks of TaN disappear and the crystal structure transfers to the Ta_2N . When the bias voltage increases further (-300 V), the Ta_2N peak tends to be wider and degenerated, implying that the grain size of the coatings gradually reduces and evolved into an amorphous structure. This result is consistent with the SEM images. It is also worth noting that the Ta_2N phase is more stable than the TaN phase under different bias voltages. Actually, the Ta_2N phase is stable in a relatively wide nitrogen concentration range and the process window is therefore wide than that of the TaN phase in the phase diagram [20]. Accordingly, it is believed that, besides the N_2 partial pressure, the bias voltage is also a significant factor that influences the phase composition of the TaN_x coatings.

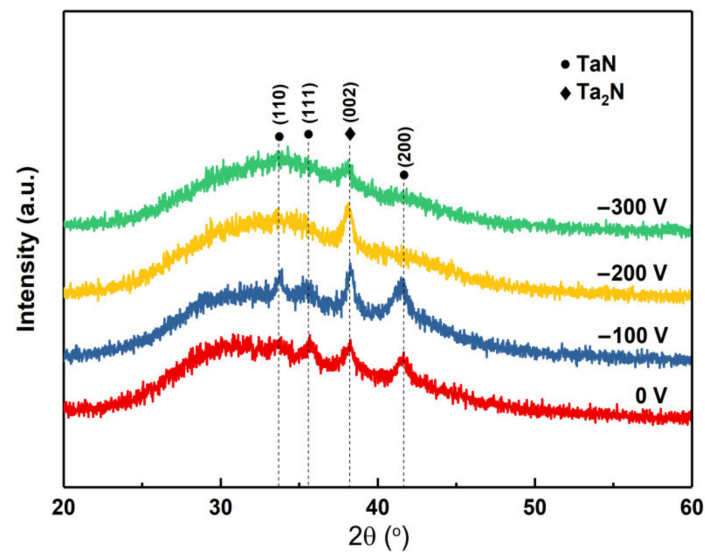


Figure 3. XRD patterns of the TaN_x coatings deposited with various bias voltages.

The surface chemical states of the coatings have been studied by XPS. The high-resolution XPS spectra for Ta 4f and N 1s are shown in Figure 4a,b. The Ta 4f peak (Figure 4a) can be deconvoluted into four peaks: Ta 4 $f_{7/2}$ peak (~ 22.7 eV), Ta 4 $f_{5/2}$ peak (~ 24.5 eV) and two peaks around 26.3 eV and 28.1 eV for Ta_2O_5 [5,12,21]. As the bias voltage increases, the peaks of Ta in the Ta_2O_5 chemical state gradually weaken, which is consistent with the compositional analysis shown in Figure 2. It should be noted that the bonding energies of the Ta 4 $f_{7/2}$ peaks (~ 22.7 eV) in the TaN_x coatings fall between that of the metallic Ta (Ta 4 $f_{7/2} \sim 21.7$ eV) and that of the standard nitride (Ta 4 $f_{7/2} \sim 23$ eV), suggesting the formation of the Ta-N bonding in a low-stoichiometry ($0 < x < 1$) chemical state. However, the result of the composition analysis above shows that the N/Ta ratio > 1 . Accordingly, it may be concluded that some N was implanted in Ta, i.e., Ta(N). As the bias voltage increases, both the Ta 4 $f_{7/2}$ and Ta 4 $f_{5/2}$ peaks shift to higher binding energy, indicating the transformation from the metal-rich state to the Ta-N bonding state. The high energy due to high bias voltage might facilitate the binding of Ta and N. The N 1s (Figure 4b) spectra are also examined. The broad peak of the N 1s spectrum can be fitted with three peaks: the peak around 402 eV representing for Ta 4 $p_{3/2}$ is almost constant, the peak centered at about 397 eV can be assigned to N in TaN, and the peak around 398 eV can be ascribed to N in Ta_2N . This depicts the presence of two binding states of TaN and Ta_2N , consistent with the results of the XRD analysis above. In addition, it is worth noting that as the bias voltage increases, the N 1s shows a slight shift to a higher binding energy, implying the increase of the Ta_2N fraction in the coatings. This also agrees well with the XRD results.

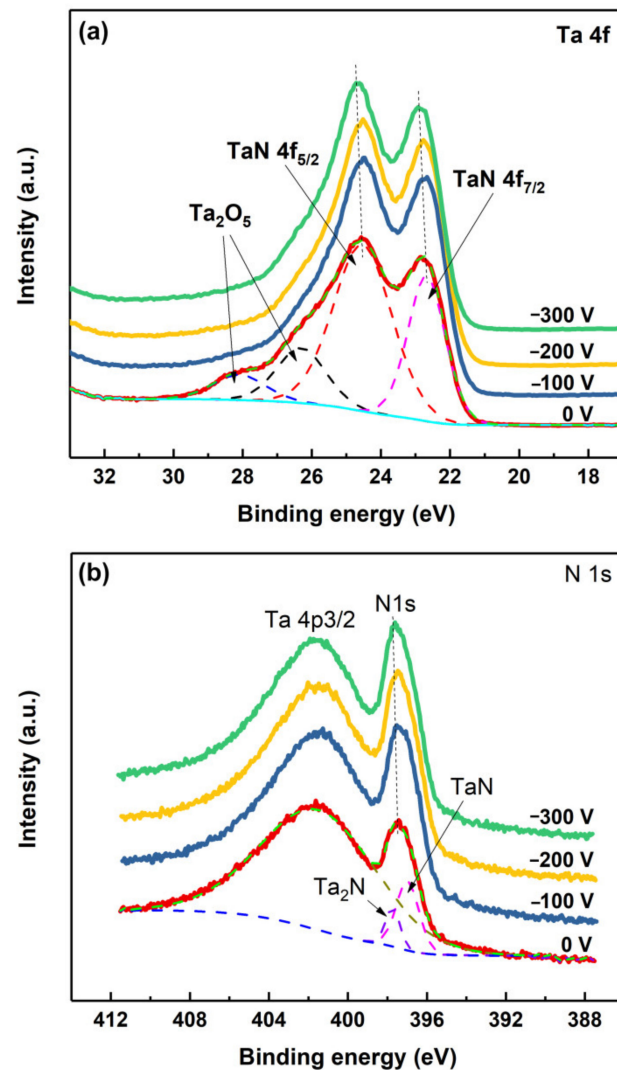


Figure 4. High resolution XPS spectra of the Ta 4f (a) and N 1s (b) of the TaN_x coatings deposited at different bias voltages.

Figure 5 presents the hardness H and the effective elastic modulus E^* of the TaN_x coatings deposited with various bias voltages. The hardness and elastic modulus of the coating deposited at 0 V are about 6 and 225 GPa, respectively. The relatively low values of hardness and elastic modulus might be attributed to the coarse and loose structure of the coating deposited with relatively low bias voltage. The coating hardness and elastic modulus are increasing with increasing bias voltage, and reach a maximum at -200 V, and then decline when the bias voltage increases further. There are conflicting factors that influence the hardness and elastic modulus of the coatings. On the one hand, as the bias voltage increases, the coarse columnar crystal is refined and the coating structure becomes compact and dense, causing the improvement of the coating hardness and elastic modulus. Furthermore, it is reported that the Ta₂N phase has higher hardness than the TaN phase [5,22]. Accordingly, the increase of the Ta₂N phase fraction with bias voltage would contribute to the improvement of the TaN_x coatings. On the other hand, the coating structure gradually transfers into an amorphous structure, resulting in the decrease of the mechanical properties of the coatings. Accordingly, the coating hardness and elastic modulus tend to decrease when the bias voltage reaches -300 V where the TaN_x coating presents an amorphous structure, as identified by the XRD. The hardness H and the effective elastic modulus E^* ratio H/E^* are also presented in Figure 5. It can be seen that the value of H/E^* increases with the bias voltage except for -100 V where the coating shows the

lowest H/E^* . The increase of the H/E^* might be attributed to the grain refinement of the coatings. High bias voltage would cause the coating structure to transfer to the zone T of the Thornton structure [23], where the coating formed exhibit dense fibrous grains with a high H/E^* ratio [24]. The H/E^* is believed to correlate with the elastic resilience and the resistance to plastic deformation, and a high H/E^* is related to a high resistance to cracking, and hence, high fracture toughness, which is beneficial to the wear resistance of the coating [25].

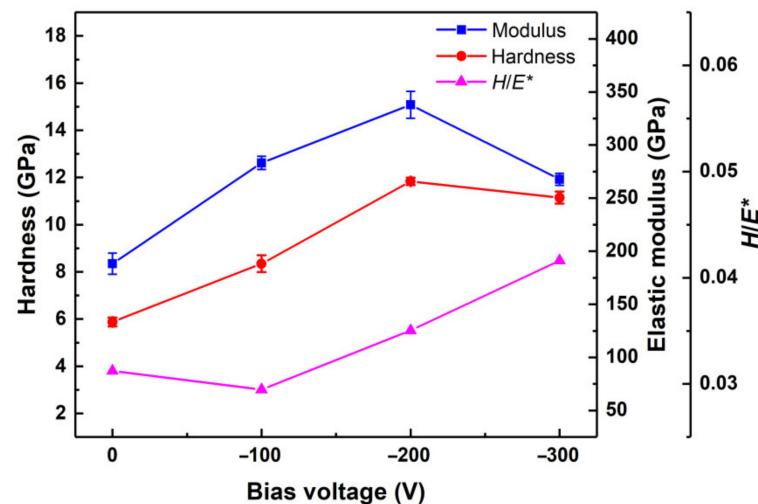


Figure 5. Hardness, elastic modulus and H/E^* of the TaN_x coatings deposited with different bias voltages.

The adhesion strength of the deposited coatings was characterized through a scratch test. The images of the scratch tracks of the coatings after the scratch test are shown in Figure 6. Usually, the critical load when the scratch begins to appear coating exfoliation (L_{c2}) is used to evaluate the coating-substrate bonding strength [26]. It can be seen that, in general, the coatings deposited with bias voltage show a relatively higher L_{c2} than that deposited without bias voltage (0 V). The TaN_x coating deposited at 0 V shows the L_{c2} of about 30 N. As the bias voltage increases, the L_{c2} of the coatings increases and reaches a maximum of about 61 N at -200 V. When the bias voltage increases further (-300 V), however, the L_{c2} of the coating tends to decrease. It is clear that an increasing bias voltage is beneficial to the adhesion of the TaN_x coatings. Significantly, the chipping and fragmentation along the edges of the scratch tracks reduce dramatically with the bias voltage. In fact, besides the coating/substrate adhesion, the detachment of the fragments is also related to the cohesive (within the coating) fraction [27]. As discussed above, the ratio H/E^* of the coatings increases with increasing bias voltage, resulting in the enhancement of the coating toughness as well as the anti-scratch performance. The critical loads of the full delamination (L_{c3}) of the coatings are also included in Figure 6. It can be seen that the variation of the L_{c3} of the coatings is similar to the L_{c2} . The maximum value occurred at a bias voltage of -200 V, implying the best adhesion of the coating is deposited at -200 V among all samples. Then the L_{c3} of the coating shows a small decrease when the bias voltage increases to -300 V. The decline of L_{c3} might be attributed to the hardness decrease of the coating deposited at -300 V.

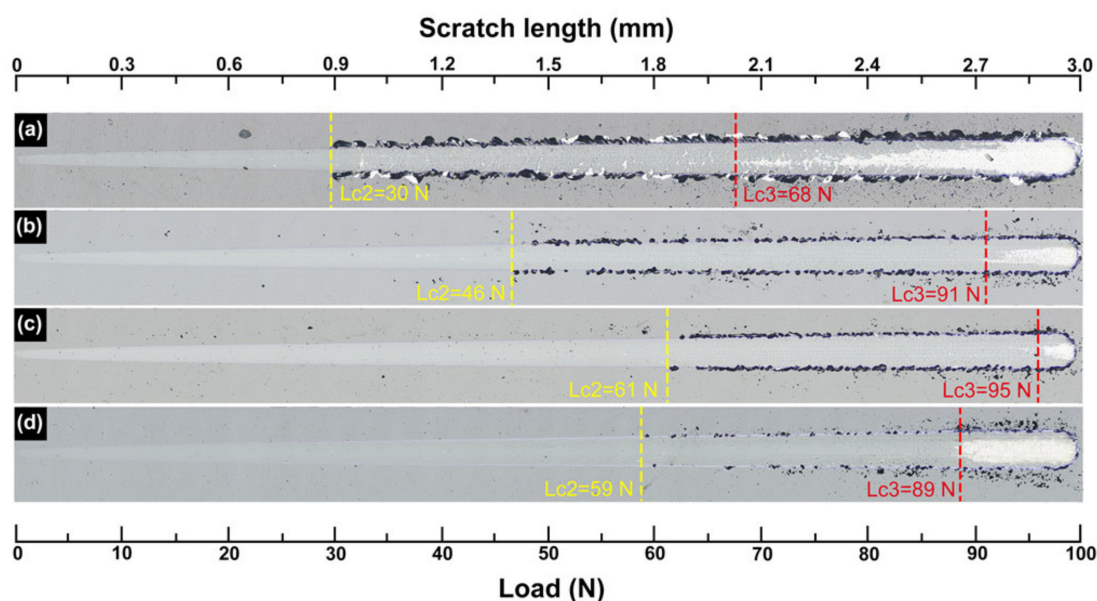


Figure 6. Typical scratch morphologies of the TaN_x coatings deposited with (a) 0 V, (b) -100 V, (c) -200 V and (d) -300 V. The corresponding critical loads of the coatings are also presented in the images.

Tribological behaviors of the deposited TaN_x coatings deposited at different bias voltages were examined with the ball-on-disk wear tester. Figure 7 presents the dynamic curves of the coefficients of friction (COFs) of the coatings as a function of friction test cycles. It can be seen that the coating deposited at -200 V presents a relative stable and smooth friction curve. The average COF is above 0.18, which is far lower than that of other PVD nitride hard coatings, e.g., CrN [28], MoN and TiN [29] which present COFs > 0.3 . For the coatings deposited with other bias voltages, the friction process can be divided into two stages after the running-in process. In the initial stage (lap < 70 cycles), all the samples show stable and low COF curves. The coatings deposited with -200 and -300 V present the lowest COF among these samples. In addition, the coating deposited at 0 V shows the maximum COF. As the lap exceeds 70 cycles, however, the friction process becomes unstable and the COF curves start to oscillate. In addition, the corresponding COFs of the coatings increase to about 0.4.

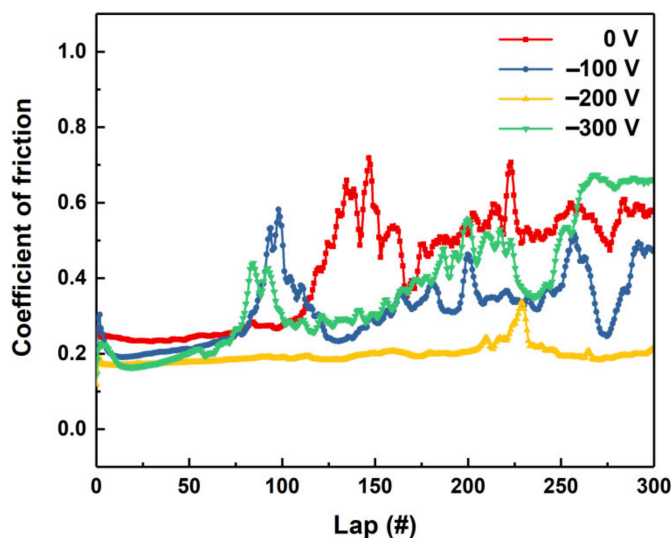


Figure 7. Dynamic curves of the friction coefficients of the TaN_x coatings deposited with various bias voltages as a function of test cycles.

The wear tracks of the samples after friction tests with 60 cycles are shown in Figure 8a–d. It should be noted that all the coatings show relatively low and smooth tracks. The wear track of the coating deposited at 0 V (Figure 8a) is deeper than that of the coatings deposited with other bias voltages, illustrating the relative higher wear rate of the coating deposited at 0 V. As the friction lap increases to 300 cycles, the wear depths of the coating increase (Figure 8e–h). It is worth noting that there is a large amount of wear debris adhered to the wear tracks on the coatings deposited at 0 and -100 V. The adherent debris might be the main reason that causes the oscillation of the friction process, as shown in the dynamic curves in Figure 7 when the lap exceeds 70 cycles. For the coating deposited with -200 V, however, the adherent debris tends to decrease and the wear track becomes shallow and narrow, implying the enhanced wear resistance of the coating. However, the wear width of the coating increases significantly when the bias voltage increases further (-300 V).

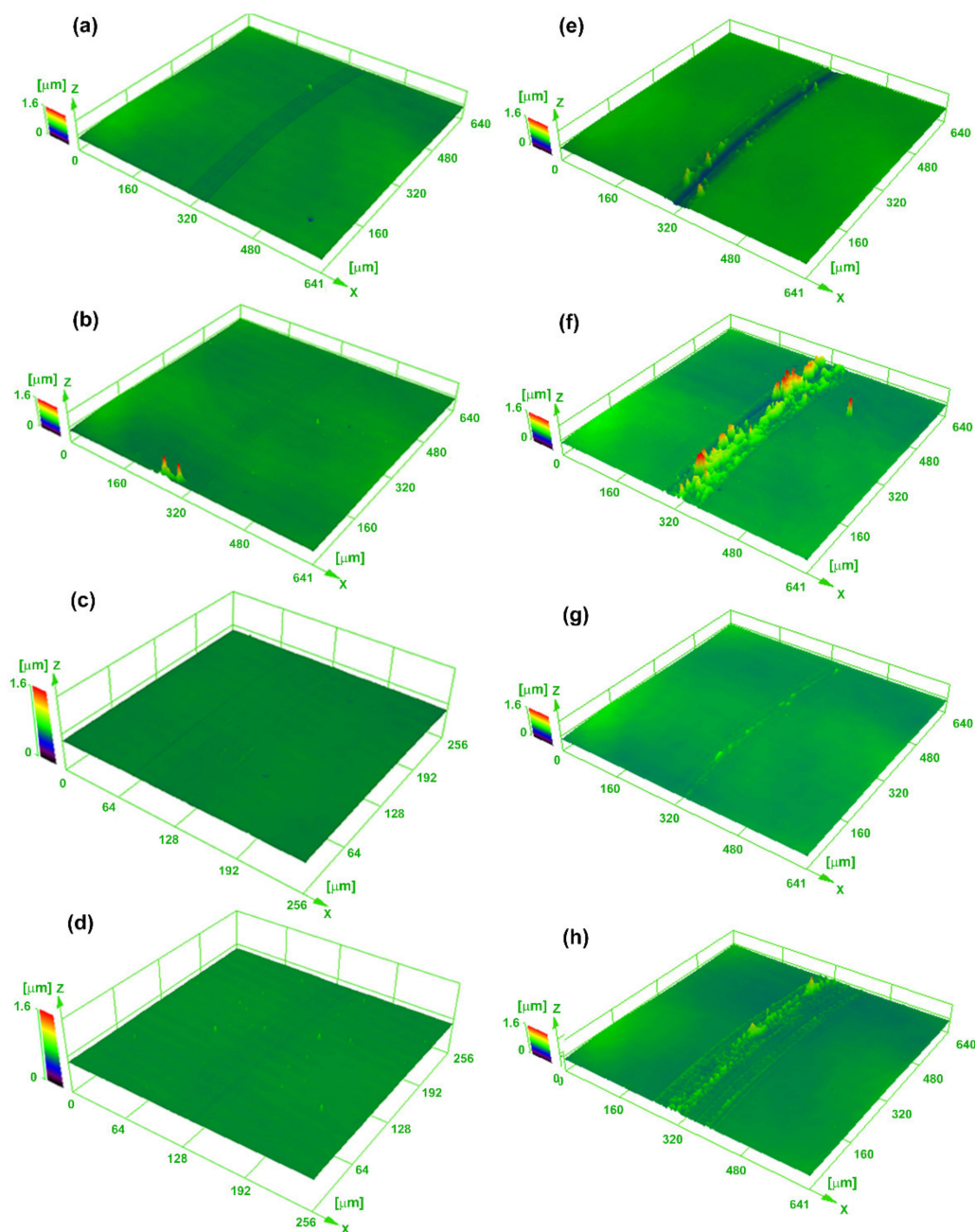


Figure 8. 3D morphologies of the wear tracks after (a–d) 60 cycles and (e–h) 300 cycles on the TaN_x coatings deposited at (a) and (e) 0 V, (b) and (f) -100 V, (c,g) -200 V and (d,h) -300 V.

Figure 9 shows a typical SEM image and the corresponding EDX mapping of the wear track of the coating deposited at -100 V. It can be seen that the wear debris adhered to the wear tracks is mainly composed of Fe (Figure 9d) and O (Figure 9c), illustrating that the wear debris was dominantly transferred from the friction SU304 ball. The relative soft SU304 can be worn away by the hard coatings. In addition, the Ta element cannot be detected in the wear track (as shown in Figure 9b), indicating that the coating peeling occurred on the wear track. The coating chipping would cause seriously abrasive wear. Accordingly, the coating deposited at -100 V exhibits a poor tribological performance.

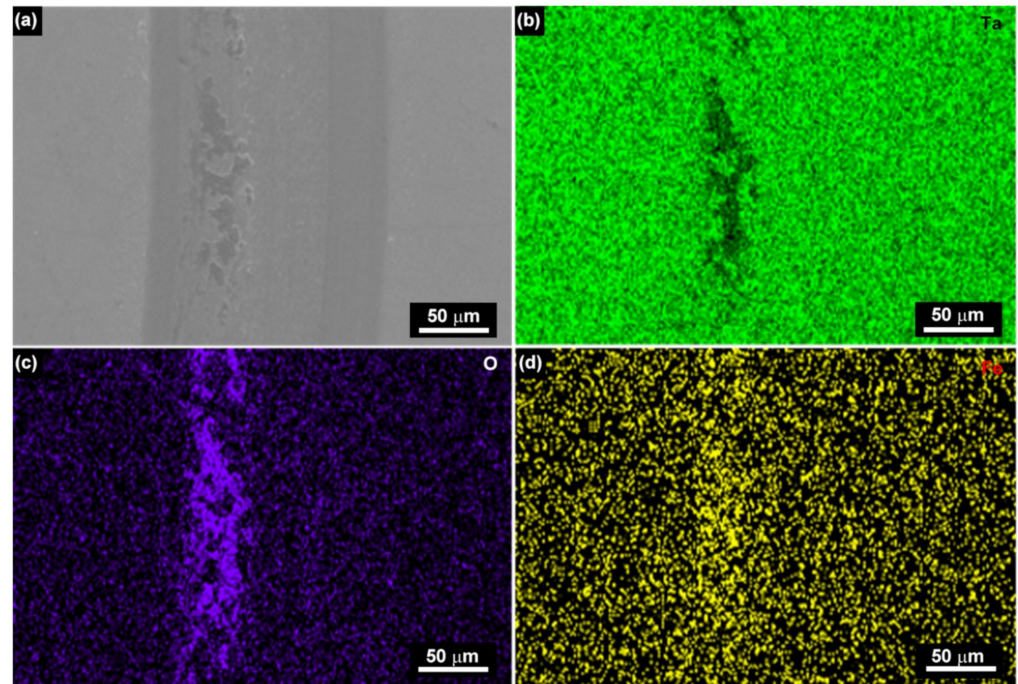


Figure 9. Typical SEM image (a) and corresponding EDX mapping (b–d) of the wear track of the coating deposited at -100 V. (b), (c) and (d) are ascribed to Ta, O and Fe, respectively.

The tribological performances of the coatings are believed to have a relationship with the composition and microstructure of the coatings. The high wear rate and COF of the coatings deposited at relative lower bias voltages (0 and -100 V) could be attributed to the presence of both TaN and Ta₂N phases, which can cause a three-body wear (e.g., the adherent wear debris) at the contact resulting in the faster wear rate [5]. In addition, the relatively low hardness and toughness (H/E^*) of the coatings also decrease the wear resistance, and the coarse surface would enhance the adhesion of the wear debris. On the contrary, the coating deposited at a relatively high bias voltage (-200 V) has a uniform microstructure that is composed of a Ta₂N phase present as fine columnar grains with enhanced hardness and smooth surface. The enhanced hardness and compact surface structure could increase the wear resistance and reduce the adhesion of the wear debris. As a result, the TaN_x coating deposited at -200 V shows a good tribological performance with low wear rate and COF. It is believed that the Ta₂N coating can serve as a potential coating material for tribological applications. However, the coating transfers into an amorphous structure as the bias voltage increases to -300 V, causing the coating hardness to decrease and then resulting in the reduction of the wear resistance.

4. Conclusions

TaN_x coatings were deposited by RF magnetron sputtering with various bias voltages. It is found that the bias voltage has a significant influence on the microstructure and composition of the TaN_x coatings. The grains of the TaN_x coatings could be refined with increasing bias voltage. The grain refinement could improve the coating hardness and

toughness. However, all the TaN_x coatings exhibited a very low ratio H/E^* (<0.042), indicating that the coating toughness is not good. The coating structure transfers from a composite structure consisting of TaN and Ta₂N crystals, through a single composite mainly composed of Ta₂N crystal, to an amorphous structure. This implies that the bias voltage is an effective way to control the phase composition of TaN_x coatings. The coating composed of Ta₂N crystal shows a good overall performance with enhanced hardness, enhanced adhesive strength and good tribological performance while the coatings consisting of TaN and Ta₂N crystals present a high wear rate due to the three-body wear. It is believed that the Ta₂N coating can serve as a potential coating material for tribological applications.

Author Contributions: W.D. planned the study and performed materials deposition and some of the characterization steps. W.D.: writing—original draft preparation, review and editing, and funding acquisition; Y.S. carried out nano-indentation, scratch test and friction test analysis. Both authors have read and agreed to the published version of the manuscript.

Funding: This work was funded by the National Natural Science Foundation of Guangdong province (Grant No. 2021A151501192).

Institutional Review Board Statement: Not applicable.

Informed Consent Statement: Not applicable.

Data Availability Statement: Not applicable.

Acknowledgments: The authors thank the financial support of the Xijiang Innovative and Entrepreneurial Team Project of Zhaoqing.

Conflicts of Interest: The authors declare that they have no known competing financial interests or personal relationships that could have appeared to influence the work reported in this paper.

References

1. Chen, S.F.; Wang, S.J.; Yang, T.H.; Yang, Z.D.; Bor, H.Y.; Wei, C.N. Effect of nitrogen flow rate on TaN diffusion barrier layer deposited between a Cu layer and a Si-Based substrate. *Ceram. Int.* **2017**, *43*, 12505–12510. [[CrossRef](#)]
2. Ma, G.; Lin, G.; Gong, S.; Liu, X.; Sun, G.; Wu, H. Mechanical and corrosive characteristics of Ta/TaN multilayer coatings. *Vacuum* **2013**, *89*, 244–248. [[CrossRef](#)]
3. Kang, S.M.; Yoon, S.G.; Suh, S.J.; Yoon, D.H. Control of electrical resistivity of TaN thin films by reactive sputtering for embedded passive resistors. *Thin Solid Films* **2008**, *516*, 3568–3571. [[CrossRef](#)]
4. Babaei, K.; Fattah-alhosseini, A.; Elmkhah, H.; Ghomi, H. Surface characterization and electrochemical properties of tantalum nitride (TaN) nanostructured coatings produced by reactive DC magnetron sputtering. *Surf. Interfaces* **2020**, *2*, 100685. [[CrossRef](#)]
5. Zaman, A.; Meletis, E.I. Microstructure and mechanical properties of TaN thin films prepared by reactive magnetron sputtering. *Coatings* **2017**, *7*, 209. [[CrossRef](#)]
6. Stampfl, C.; Freeman, A.J. Stable and metastable structures of the multiphase tantalum nitride system. *Phys. Rev. B* **2005**, *71*, 024111. [[CrossRef](#)]
7. Lee, G.R.; Kim, H.; Choi, H.S.; Lee, J.J. Superhard tantalum-nitride films formed by inductively coupled plasma-assisted sputtering. *Surf. Coat. Technol.* **2007**, *201*, 5207–5210. [[CrossRef](#)]
8. Shin, C.S.; Kim, Y.W.; Gall, D.; Greene, J.E.; Petrov, I. Phase composition and microstructure of polycrystalline and epitaxial TaN_x layers grown on oxidized Si(001) and MgO(001) by reactive magnetron sputter deposition. *Thin Solid Films* **2002**, *402*, 172–182. [[CrossRef](#)]
9. Yang, Y.H.; Chen, D.J.; Wu, F.B. Microstructure, hardness, and wear resistance of sputtering TaN coating by controlling RF input power. *Surf. Coat. Technol.* **2016**, *303*, 32–40. [[CrossRef](#)]
10. Rudolph, M.; Lundin, D.; Foy, E.; Debongnie, M.; Hugon, M.C.; Minea, T. Influence of backscattered neutral on the grain size of magnetron-sputtered TaN thin films. *Thin Solid Films* **2018**, *658*, 46–53. [[CrossRef](#)]
11. Mendizabal, L.; Bayón, R.; G-Berasategui, E.; Barriga, J.; Gonzalez, J.J. Effect of N₂ flow rate on the microstructure and electrochemical behavior of TaN_x films deposited by modulated pulsed power. *Thin Solid Films* **2016**, *610*, 1–9. [[CrossRef](#)]
12. Kuo, Y.L.; Huang, J.J.; Lin, S.T.; Lee, C.; Lee, W.H. Diffusion barrier properties of sputtered TaN_x between Cu and Si using TaN as the target. *Mater. Chem. Phys.* **2003**, *80*, 690–695. [[CrossRef](#)]
13. Valdez, K.; Espinosa-Arbeláez, D.G.; García-Herrera, J.E.; Muñoz-Saldaña, J.; Farias, M.H.; De la Cruz, W. Influence of substrate temperature and N₂/Ar flow ratio on the stoichiometry, structure and hardness of TaN_x coatings deposited by DC reactive sputtering. *Surf. Interface Anal.* **2015**, *47*, 1015–1019. [[CrossRef](#)]
14. Liu, E.; Jin, G.; Cui, X.; Xiao, Q.; Shao, T. Effect of gas pressure on the mechanical properties of sputtered TaN films. *Phys. Procedia* **2013**, *50*, 438–441. [[CrossRef](#)]

15. Tan, S.; Zhang, X.; Wu, X.; Fang, F.; Jiang, J. Comparison of chromium nitride coatings deposited by DC and RF magnetron sputtering. *Thin Solid Films* **2011**, *519*, 2116–2120. [[CrossRef](#)]
16. Li, T.C.; Lwo, B.J.; Pu, N.W.; Yu, S.P.; Kao, C.H. The effects of nitrogen partial pressure on the properties of the TaN_x films deposited by reactive magnetron sputtering. *Surf. Coat. Technol.* **2006**, *201*, 1031–1036. [[CrossRef](#)]
17. Anders, A. A structure zone diagram including plasma-based deposition and ion etching. *Thin Solid Films* **2010**, *528*, 4087. [[CrossRef](#)]
18. Meymian, M.R.Z.; Heravi, A.D.; Mehr, A.K. Influence of bias voltage on optical and structural characteristics of Cu₃N films deposited by reactive RF magnetron sputtering in a pure nitrogen atmosphere. *Mater. Sci. Semicon. Proc.* **2020**, *112*, 104995. [[CrossRef](#)]
19. Kim, S.K.; Cha, B.C. Deposition of tantalum nitride thin films by D.C. magnetron sputtering. *Thin Solid Films* **2005**, *475*, 202–207. [[CrossRef](#)]
20. Riekkinen, T.; Molarius, J.; Laurila, T.; Nurmela, A.; Suni, I.; Kivilahti, J.K. Reactive sputter deposition and properties of TaN thin films. *Microelectron. Eng.* **2002**, *64*, 289–297. [[CrossRef](#)]
21. Liu, X.; Ma, G.J.; Sun, G.; Duan, Y.P.; Liu, S.H. Effect of deposition and annealing temperature on mechanical properties of TaN film. *Appl. Surf. Sci.* **2011**, *258*, 1033–1037. [[CrossRef](#)]
22. Westergård, R.; Bromark, M.; Larsson, M.; Hedenqvist, P.; Hogmark, S. Mechanical and tribological characterization of DC magnetron sputtered tantalum nitride thin films. *Surf. Coat. Technol.* **1997**, *97*, 779–784. [[CrossRef](#)]
23. Thornton, J. Recent developments in sputtering-magnetron sputtering. *Met. Finish.* **1979**, *775*, 83–87.
24. Musil, J. Flexible hard nanocomposite coatings. *RSC Adv.* **2015**, *5*, 60482–60495. [[CrossRef](#)]
25. Musil, J. Hard nanocomposite coatings: Thermal stability, oxidation resistance and toughness. *Surf. Coat. Technol.* **2012**, *207*, 50–65. [[CrossRef](#)]
26. Randall, N.X. The current state-of-the-art in scratch testing of coated systems. *Surf. Coat. Technol.* **2019**, *380*, 125092. [[CrossRef](#)]
27. Sveen, S.; Andersson, J.M.; M'saoubi, R.; Olsson, M. Scratch adhesion characteristics of PVD TiAlN deposited on high speed steel, cemented carbide and PCBN substrates. *Wear* **2013**, *308*, 133–141. [[CrossRef](#)]
28. Lin, J.; Sproul, W.D.; Moore, J.J.; Lee, S.; Myers, S. High rate deposition of thick CrN and Cr₂N coatings using modulated pulse power (MPP) magnetron sputtering. *Surf. Coat. Technol.* **2011**, *205*, 3226–3234. [[CrossRef](#)]
29. Öztürk, A.; Ezirmik, K.V.; Kazmanlı, K.; Ürgen, M.; Eryılmaz, O.L.; Erdemir, A. Comparative tribological behaviors of TiN-, CrN- and MoN-Cu nanocomposite coatings. *Tribol. Int.* **2008**, *41*, 49–59. [[CrossRef](#)]